ADVANCED MATERIALS
www.advmat.de

Fabrication of Millimeter-Scale, Single-Crystal One-Third-Hydrogenated Graphene with Anisotropic Electronic Properties

Hui Chen, De-Liang Bao, Dongfei Wang, Yande Que, Wende Xiao, Guojian Qian, Hui Guo, Jiatao Sun, Yu-Yang Zhang, Shixuan Du, Sokrates T. Pantelides, and Hong-Jun Gao**

Periodically hydrogenated graphene is predicted to form new kinds of crystalline 2D materials such as graphane, graphone, and 2D C_xH_y, which exhibit unique electronic properties. Controlled synthesis of periodically hydrogenated graphene is needed for fundamental research and possible electronic applications. Only small patches of such materials have been grown so far, while the experimental fabrication of large-scale, periodically hydrogenated graphene has remained challenging. In the present work, large-scale, periodically hydrogenated graphene is fabricated on Ru(0001). The as-fabricated hydrogenated graphene is highly ordered, with a $\sqrt{3} \times \sqrt{3}$/R30° period relative to the pristine graphene. As the ratio of hydrogen and carbon is 1:3, the periodically hydrogenated graphene is named "one-third-hydrogenated graphene" (OTHG). The area of OTHG is up to 16 mm^2. Density functional theory calculations demonstrate that the OTHG has two deformed Dirac cones along one high-symmetry direction and a finite energy gap along the other directions at the Fermi energy, indicating strong anisotropic electrical properties. An efficient method is thus provided to produce large-scale crystalline functionalized graphene with specially desired properties.

Chemical modification of graphene is a key tool to fabricate a wide range of graphene-based materials.[1–8] In particular, hydrogenation of graphene creates local geometric distortions by changing the C hybridization from sp^2 to sp^3,[9] enhances graphene's spin–orbit coupling (SOC),[10] introduces a finite bandgap,[11] and generates magnetic moments.[12] In hydrogenated graphene, hydrogen coverages and distributions have been found to substantially alter the electronic properties of graphene.[13,14] Thus, the absence of uniformity in the distribution of H atoms leads to difficulties in practical device designs. In contrast, large-scale periodically hydrogenated graphene, namely, with hydrogen atoms chemisorbed in a uniformly periodic manner, are effectively new kinds of 2D crystalline materials, such as graphane,[15] graphone,[16] and 2D C_xH_y.[17–20] These crystalline graphene derivatives have been predicted to exhibit unique electronic properties beyond pristine graphene, such as large bandgap,[15] ferromagnetism,[16,20] and strong optical absorption.[17]

The first experimental work on the fabrication of periodically hydrogenated graphene was reported by Elias et al. in 2009.[9] Electron diffraction in a transmission electron microscope (TEM) demonstrated that the hydrogenated freestanding graphene is crystalline and the most likely candidate is graphane.[9] The authors noted that the samples are nonuniform and attributed the discrepancy to the possibility that the experimentally produced graphane might have a more complex hydrogen bonding than the one suggested by theory.[9] The size of uniform patches of hydrogenated graphene was not reported.[9] More recently, there has been significant progress in the synthesis of hydrogenated graphene.[11,21–26] Haberer et al. reported the fabrication of graphone and used X-ray photoelectron spectroscopy (XPS) to determine the H/C stoichiometry.[21] Islands of $\sqrt{3} \times \sqrt{3}$/R30°-phased hydrogenated graphene have been fabricated using the scanning tunneling microscope (STM) tip-induced field dissociation of H_2 on a scale of ≈70 nm.[22] Moreover, many samples with small patches of locally ordered hydrogenated graphene have been fabricated.[11,23–26] As the first step toward potential large-scale applications, seeking methods to fabricate millimeter-scale periodically hydrogenated graphene with a specific carbon/hydrogen ratio is still an open challenge.

In the present work, we report millimeter-scale fabrication of single-crystal one-third-hydrogenated graphene on Ru(0001). Graphene/Ru(0001)[27,28] is adopted as the growth template

Dr. H. Chen, D.-L. Bao, D. Wang, Dr. Y. Que, Prof. W. Xiao, G. Qian, H. Guo, Prof. J. Sun, Prof. Y.-Y. Zhang, Prof. S. Du, Prof. S. T. Pantelides, Prof. H.-J. Gao
Institute of Physics and School of Physical Sciences and CAS Center for Excellence in Topological Quantum Computation
University of Chinese Academy of Sciences
Chinese Academy of Sciences
Beijing 100190, China
E-mail: sxdu@iphy.ac.cn; hjgao@iphy.ac.cn
D.-L. Bao, Prof. Y.-Y. Zhang, Prof. S. T. Pantelides
Department of Physics and Astronomy and Department of Electrical Engineering and Computer Science
Vanderbilt University
Nashville, TN 37235, USA

DOI: 10.1002/adma.201801838

because of the high-quality, large-scale, single-crystal graphene that has served well as a template for the adsorption of atoms[29,30] or molecules.[31] We show that the sample exhibits a moiré pattern with a periodicity of ≈25.4 Å after cycles of hydrogen adsorption and subsequent annealing. Raman spectra indicate the formation of hydrogenated graphene with weak interaction with the substrate. We demonstrate that the hydrogen atoms are arranged in a $\sqrt{3} \times \sqrt{3}$/R30° superstructure with respect to the graphene lattice and chemisorbed on both sides of the graphene plane. Low-energy electron diffraction (LEED) combined with STM images demonstrate that the single-crystal OTGH sample has areas up to 16 mm^2. We also find that, the hydrogen atoms initially prefer to adsorb on the atop regions of graphene on Ru(0001). As the hydrogen dosage is increased, the $\sqrt{3} \times \sqrt{3}$/R30° superstructure extends from the atop regions to the whole graphene sheet and finally forms large-scale periodic structures. Moreover, dI/dV spectra exhibit the typical V-shape dip instead of bandgap around the Fermi energy. Calculations demonstrate that the freestanding OTHG has two tilted Dirac cones at the Fermi energy along one high-symmetry direction but a finite energy gap along other directions. The unique band structures of OTHG are originating from the selective hydrogen adsorption, suggesting strong anisotropic properties of this new 2D material.

The hydrogenated graphene was fabricated through several cycles of exposure of a monolayer graphene (MLG) on Ru(0001) to atomic hydrogen generated by a radio-frequency (RF) atom source and subsequent annealing (**Figure 1**a). One cycle refers to exposing the MLG to atomic hydrogen for 20 min at ≈150 °C and subsequently annealing to ≈900 °C for 20 min. Figure 1b shows two LEED patterns before and after four cycles of hydrogen exposure, respectively. A $\sqrt{3} \times \sqrt{3}$/R30° superstructure with respect to the graphene lattice, induced by hydrogenation, is observed, indicating the formation of periodically hydrogenated graphene. Figure 1c shows a large-scale (250 nm × 250 nm) STM image of the hydrogenated MLG on a Ru(0001) after four cycles of hydrogen adsorption. The periodic meshes in the STM image and corresponding fast Fourier transformation (FFT) pattern indicate the formation of a well-ordered hexagonal superstructure induced by atomic hydrogen adsorption. A control experiment where the graphene was subjected to annealing and RF without hydrogen dose shows that there are no structural changes (Figure S1, Supporting Information).

The periodically hydrogenated graphene is proved to be weakly coupled with the substrate. Figure 1d shows the Raman spectra of graphene on Ru(0001) before and after hydrogenation. Prior to hydrogenation, the Raman spectrum of MLG/Ru is essentially featureless (the red curve), which is due to the hybridization of the π-electrons of graphene and the Ru 4d state.[32,33] In contrast, after four cycles of atomic hydrogen dosage, the Raman spectrum is characteristic of a partially hydrogenated MLG, including G and 2D bands, indicating a significant weakening of the coupling between the hydrogenated graphene and the metal substrate.[34,35] The emerging of the D′ band, the high intensity of the defect-associated graphene D band, and the broadening of the G band indicate the breaking of the translational symmetry of C=C sp^2 bonds and the formation of C−H sp^3 bonds after hydrogenation.[9]

The atomic configuration of the as-fabricated hydrogenated graphene is confirmed by a combination of STM images, FFT patterns, Raman measurements, and density functional theory (DFT) calculations. **Figure 2**a shows a zoom-in STM image of Figure 1c, showing that the hexagonal superstructure is a moiré pattern with a periodicity of 25.4 ± 1.5 Å. A zoom-in of Figure 2a shows a hexagonal structure with a lattice constant of 4.3 ± 0.2 Å (blue dashed rhombus in Figure 2b). By moving the scanning tip close to the sample (sample bias: −2 mV; tunneling current: 1.0 nA), we get a further zoom-in STM image of the hexagonal lattice as shown in Figure 2c, where the hexagonal lattice is resolved into ordered arrays of 1D sawtooth-shaped stripes. In the FFT pattern of the STM image (inset in

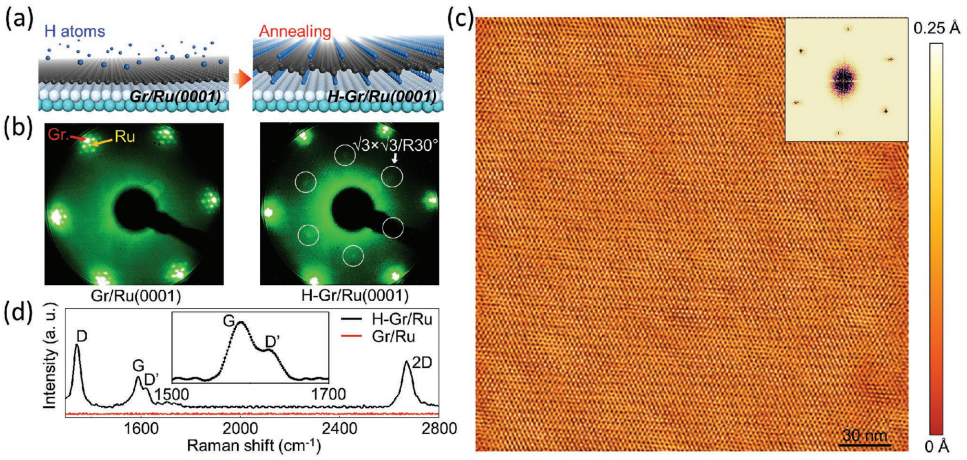

Figure 1. Large-scale synthesis of periodically hydrogenated graphene on Ru(0001). a) Schematic showing the fabrication of periodically hydrogenated graphene on Ru(0001) through atomic hydrogen chemisorption. b) LEED pattern of graphene (left panel) and hydrogenated graphene (right panel) on Ru(0001). The red and yellow arrows indicate the diffraction spots from graphene and Ru(0001), respectively. The white circles indicate the $\sqrt{3} \times \sqrt{3}$/R30° with respect to graphene induced by hydrogenation. The beam energy is 69 eV. c) A large-scale STM image of hydrogenated graphene on Ru(0001) and corresponding fast Fourier transformation (FFT) of the image (inset), showing the formation of hexagonal patterns (Sample bias: U = −20 mV, Tunneling current: I = 0.2 nA). d) Raman spectra of graphene (red curve) and periodically hydrogenated graphene (black curve) on Ru(0001), showing the recovery of the G peak and 2D peak. The inset shows a high-resolution spectrum of the G and D′ band of hydrogenated graphene.

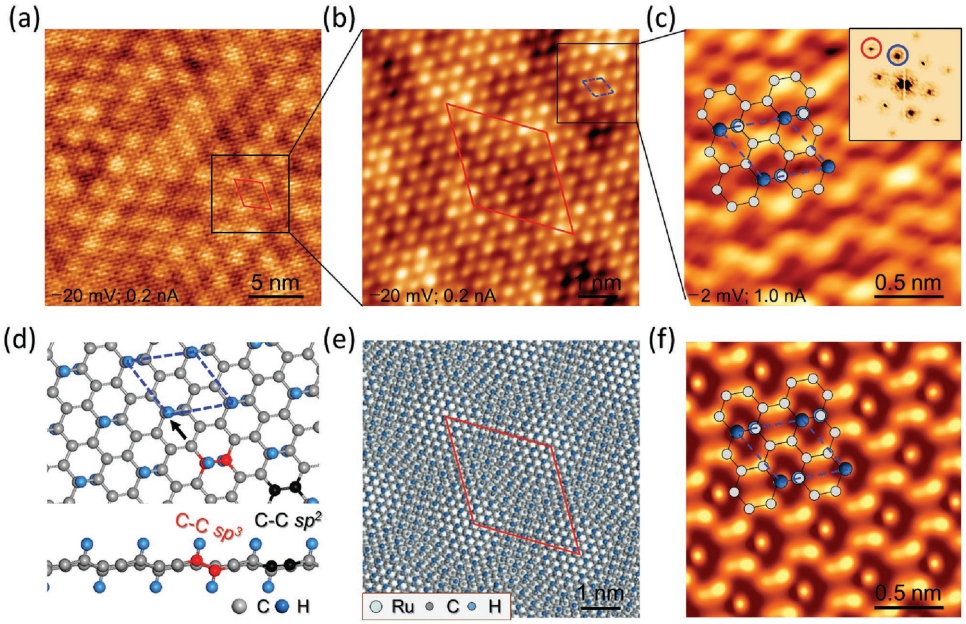

Figure 2. Atomic configuration of the OTHG on Ru(0001). a) A relatively large STM image of as-fabricated hydrogenated graphene, showing a hexagonal lattice modulated by a moiré pattern with a periodicity of 25.4 ± 1.5 Å ($U = -20$ mV, $I = 0.2$ nA), marked by the red rhombus. b) Zoom-in STM image of the area marked by black box in (a), showing a hexagonal lattice with a periodicity of 4.3 ± 0.2 Å ($U = -20$ mV; $I = 0.2$ nA), marked by the blue dashed rhombus. The red solid rhombus represents the period of the moiré pattern. c) Zoom-in STM image of the area marked by black box in (b), using different scanning parameters ($U = -2.0$ mV; $I = 1.0$ nA), showing ordered arrays of 1D sawtooth-shaped stripes. The inset displays the FFT pattern corresponding to the graphene lattice (outer set of spots, marked by red circles) and superstructure induced by hydrogen adsorption (inner set of spots, marked by blue circles). The $\sqrt{3} \times \sqrt{3}$/R30° hydrogen adsorbate structures are superimposed on the STM image. d) Top view and side view, looking along the direction indicated with a black arrow, of a freestanding OTHG showing a double-sided $\sqrt{3} \times \sqrt{3}$/R30° hydrogen-adsorbed structure. Two of the hydrogenated C atoms are highlighted with red color, representing that hydrogenated C atoms move out of the plane with C—C sp^3 bonding. Two of the unhydrogenated C atoms are highlighted with black color, representing that unhydrogenated C atoms are almost planar with C—C sp^2 bonding. e) A schematic top view of the moiré superlattice of OTHG grown on Ru(0001). The unit cell of the moiré superlattice with a periodicity of 25.4 Å is highlighted with red rhombus. f) Simulated STM images of OTHG at the bias of −1.0 eV relative to the Fermi energy. The $\sqrt{3} \times \sqrt{3}$/R30° hydrogen adsorbate structures are superimposed on the image, showing excellent agreement with the experimental STM images.

Figure 2c), two sets of spots can be identified. By measuring the lengths between two neighboring spots in each set, we confirm that the outer set of spots (red circles in inset of Figure 2c) correspond to the graphene lattice (2.46 Å), while the inner set of spots (blue circles in inset of Figure 2c) are assigned to that of hexagonal superstructures induced by hydrogen adsorption (4.30 Å). The lattice constant of the hydrogen adsorbate structure, 4.3 Å, is about $\sqrt{3}$ times the lattice constant of pristine graphene (2.46 Å). A rotation angle of ≈30° between the two sets of spots is evaluated. The STM images and related FFT patterns demonstrate that the as-fabricated hydrogenated graphene is a $\sqrt{3} \times \sqrt{3}$/R30° superstructure relative to the pristine graphene lattice, which agree with the LEED measurements.

The quasi-freestanding features in the Raman spectra of hydrogenated graphene (Figure 1d) suggest the existence of hydrogen atoms in the interface between graphene and Ru substrate. Furthermore, the as-fabricated hydrogenated graphene structure on Ru(0001) is very stable in the air for more than 30 d (Figure S2, Supporting Information). It is also stable upon annealing up to 900 °C for several hours in vacuum, which is different from the recovering of pristine graphene from hydrogenated graphene on other substrates[11,21] via dehydrogenation at elevated temperature. It has been reported that hydrogen atoms on both sides of a graphene sheet are energetically preferred over having the hydrogen atoms on a single side, that is, double-sided-hydrogenated graphene has higher thermal stability than single-side-hydrogenated graphene.[36,37] For the above reasons, we infer that the as-fabricated material is a double-sided-hydrogenated graphene.

To further explore the atomic configuration of the as-prepared hydrogenated graphene, we performed DFT calculations based on the model of a freestanding double-sided-hydrogenated graphene with a $\sqrt{3} \times \sqrt{3}$/R30° superstructure relative to the pristine graphene, as shown in Figure 2d. The unit cell contains six carbon atoms and two hydrogen atoms that bond to two neighboring C atoms on both sides, corresponding to an OTHG structure. We find that this OTHG is buckled. The hydrogenated C atoms (representative C atoms are highlighted with red color in Figure 2d) move higher and lower, respectively, with a C—C sp^3 bond length of 1.53 Å. The C atoms without hydrogen atom bonding (representative C atoms are highlighted with black color in Figure 2d) are almost planer with a C—C sp^2 bond length of 1.39 Å (Figure 2d). The calculated periodicity of the OTHG is 4.27 Å, in good agreement with the experimental value, 4.3 Å. The hydrogen atoms are slightly shifted toward the center of the C—C bonds. The moiré superstructure in the experimental images (Figure 2b), whose periodicity is 25.4 Å, is schematically described by a 10×9 model (10×10 graphene sitting on 9×9 Ru(0001) substrate), as shown in Figure 2e. Figure 2f

shows a STM simulation that reproduces the STM image in Figure 2c very well.

We also calculated the formation energy of OTHG. Comparing with the fully hydrogenated graphene (graphane), OTHG is more stable at hydrogen-poor conditions (see Figure S3, Supporting Information, for more discussion). In addition, we did ab initio molecular dynamics (AIMD) simulations to test the stability of OTHG (see Movie S1, Supporting Information) at 1200 K (927 °C) for 7 ps. We did not observe hydrogen desorption, indicating the OTHG is stable at this temperature.

We found that OTHG has formed continuously over a very large area of 16 mm^2 on the Ru surface, as indicated by the sharp LEED patterns shown in Figure S4 (Supporting Information). The sample was moved continuously, and individual LEED patterns at different locations were obtained across the surface at 0.67 mm intervals. Five examples of LEED patterns are shown in Figure S4 (Supporting Information). They all show additional spots with the same arrangement, indicating single-crystalline OTHG is formed at these locations. The series of large-scale and atomically resolved STM images taken from random areas shows crystalline OTHG structures with the same orientations (Figure S5, Supporting Information). A high-resolution STM image taken over the step shows that the OTHG structure on the upper terrace extends continuously to the lower terrace (Figure S5, Supporting Information). The size of a single-crystal OTHG sample in this work is much larger than the size of continuous single-crystal periodically hydrogenated graphene island in previous reports (see Table S1, Supporting Information).

To investigate the growth process of OTHG on Ru(0001), we acquired a series of STM images during the growth. **Figure 3**a,e shows STM images of high-quality MLG on a Ru(0001) before hydrogenation. The MLG exhibits a regular moiré pattern with a periodicity of ≈30 Å due to the lattice mismatch between graphene and Ru(0001) surface (marked by blue rhombus in Figure 3e).[24] Three different regions, namely, atop, fcc, and hcp regions, can be distinguished in each unit cell of this moiré pattern. After one cycle (20 min) of hydrogen dosage, we found that there are some morphological changes in the moiré pattern of graphene/Ru, as shown in Figure 3b. Figure 3f is a zoom-in STM image of Figure 3b, showing that the atop regions are significantly distorted and broadened. We attribute the distortion and broadening of atop regions to hydrogen adsorption. In contrast, there are only minor morphological changes in the fcc and hcp regions. These results suggest that hydrogen atoms are preferentially anchored at the atop regions of the moiré pattern of graphene/Ru in the initial growth stage.

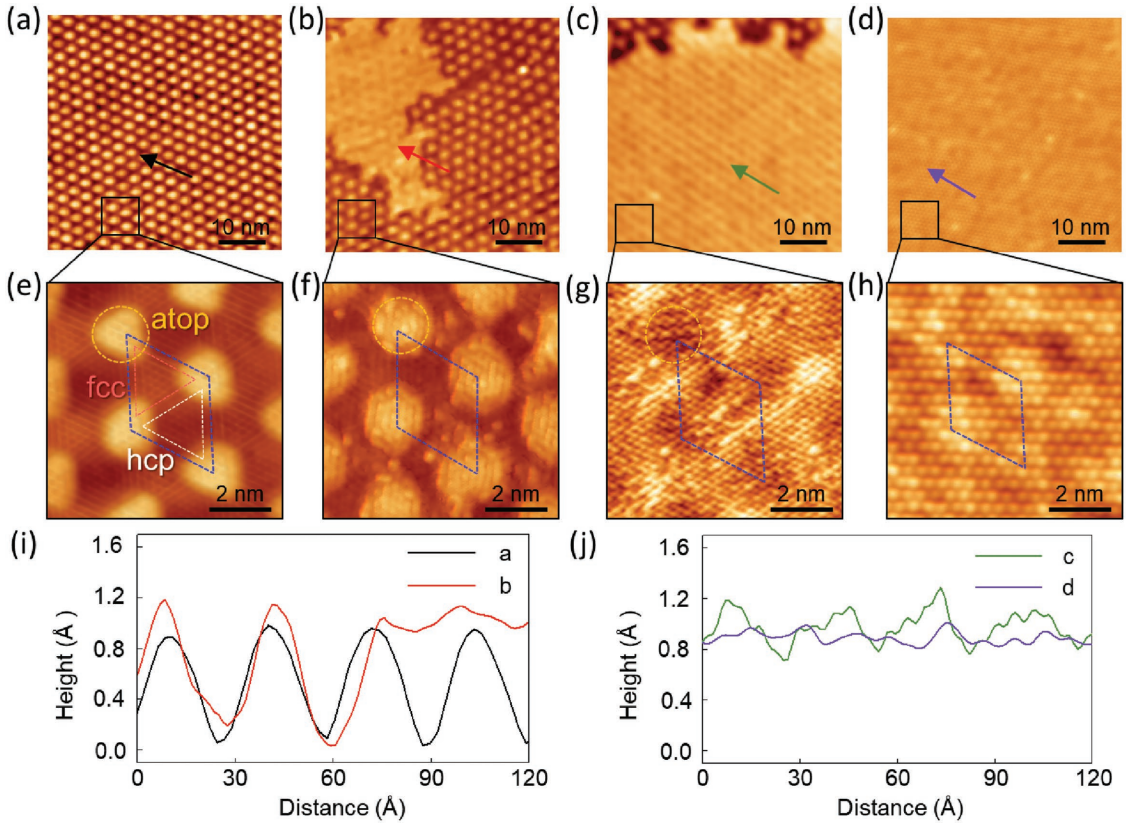

Figure 3. Structural evolution in the growth process of OTHG on Ru(0001). a–d) STM images of graphene exposed to atomic hydrogen for 0, 20, 40, and 80 min, respectively, showing the morphological evolution with increasing hydrogen dosage ($U = -200$ mV, $I = 0.01$ nA). e–h) High-resolution STM images in the black boxes of (a)–(d), respectively, showing the evolution of atomic structures and moiré patterns with increasing hydrogen dosage. The moiré pattern of each superstructure is marked by blue rhombus ($U = -20$ mV, $I = 0.1$ nA). i) Lateral line profiles along the black and red arrows in (a) and (b), respectively. j) Lateral line profiles along the green and purple arrows in (c) and (d), respectively. The data in (i) and (j) indicate that the corrugation in sample is decreased as the hydrogen dosage is increased.

We also noted that there is a small flat area surrounded by the moiré pattern in Figure 3b. We plotted the line profiles (Figure 3i) along the back arrow in Figure 3a and red arrow in Figure 3b, respectively. The corrugation of the moiré pattern area (left part of red curve) is about 1.0 Å, similar to that of the pristine graphene/Ru (black curve). On the other hand, the corrugation of the flat area is merely 0.4 Å (right part of the red curve), much smaller than that of the moiré pattern area. The results indicate that more hydrogen atoms adsorb in the hcp and fcc regions of flat areas, leading to the uplift of fcc and hcp regions and the decrease in the corrugation. The uplift is consistent with the notion that some hydrogen atoms are intercalated between graphene and the Ru substrate in the growth process of a double-sided-hydrogenated graphene.[38,39]

With increasing hydrogen dosage (2 cycles, 40 min), as shown in Figure 3c, the flat areas almost extend to the whole surface. High-resolution STM image of flat areas (Figure 3g) exhibits a moiré superstructure with a periodicity of 28 Å (marked by blue rhombus), which is slightly smaller than that of pristine graphene/Ru. At atop regions of the moiré superstructure in the flat area (indicated by the yellow dotted circle), ordered arrays consisting of 1D sawtooth-shaped stripes with a periodicity of 4.3 ± 0.2 Å corresponding to an OTHG structure are observed. In contrast, the OTHG structure cannot be found in the fcc and hcp regions, suggesting that OTHG initially forms at the atop regions of the moiré pattern of pristine graphene/Ru during growth.

With a further increase of hydrogen dosage (4 cycles, 80 min), the OTHG structures expand from the atop regions to the whole graphene sheet, as shown in Figure 3d,h. We found that the surface becomes extremely flat in the STM image after the expansion of the OTHG structure. Figure 3j shows the line profiles along the green arrow in Figure 3c and purple arrow in Figure 3d, respectively. The corrugation of the moiré superstructure of OTHG is about 0.25 Å (purple curve), smaller than that of flat areas in the former growth step (0.4 Å, green curve). With extensive adsorption, we noted that the OTHG structure in some regions will be gradually broken into disordered structure, indicating that the quality of OTHG decreased (Figure S6, Supporting Information).

To study the electronic properties of the new 2D material OTHG, we collected dI/dV spectra on the OTHG. As **Figure 4**a shows, there is no energy gap, but a V-shape Dirac cone around the Fermi level (E_F), which is different from the previous reports that an energy gap is opened around E_F induced by hydrogen chemisorption.[11,25] To get a better understanding of the dI/dV spectra, we calculated the energy bands of the OTHG configuration in Figure 2d. The first Brillouin zone (BZ) and calculated band structure are shown in Figure 4b,c, respectively. The calculated band structure shows that there are two distorted Dirac cones at E_F along the Γ-M2 and Γ-M5 directions, perpendicular to the direction running along the sawtooth-shaped stripes in the STM images (Figure 2f). Moreover, the band structure along the other directions shows substantial bandgaps (about 0.6 eV). The calculated total density of states (DOS) of OTHG show a typical V-shape at E_F (right panel of Figure 4c), demonstrating the existence of a Dirac cone, in agreement with the dI/dV spectra recorded on OTHG. The band structure in Figure 4c is in agreement with the published result[18] (here we used the HSE06 hybrid functional method to obtain more accurate energy bands). Considering the significant anisotropic electronic structure, we anticipate that the as-prepared OTHG exhibits novel anisotropic physical properties, for example, anisotropic Fermi velocity, directional conductance, and anisotropic mechanical properties.[40]

We noted that Lin and co-workers have conducted theoretical calculations of similar hydrogenated graphene structures, where the hydrogenated graphene has an energy gap of ≈0.6 eV and lacks a Dirac cone.[22] This disagreement might result from their exclusion of the Γ-M2 path in the energy-band plots.

In summary, we fabricated a periodically hydrogenated graphene, OTHG, on Ru(0001) at a millimeter scale by exposing MLG to atomic hydrogen induced by a RF atom source. LEED and STM images confirm the formation of single-crystal periodically hydrogenated graphene at a millimeter scale. The adsorption of hydrogen atoms leads to the formation of a crystalline hydrogenated structure that exhibits a moiré pattern with a periodicity of ≈25.4 Å. The hydrogen atoms are adsorbed on both sides of the graphene sheet and are arranged in a $\sqrt{3} \times \sqrt{3}$/R30° superstructure with respect to the graphene lattice, resulting in an OTHG structure. The OTHG interacts weakly with the Ru substrate and is structurally anisotropic. The structural anisotropy results in an anisotropic electronic structure, rendering the as-fabricated OTHG a candidate for future applications requiring anisotropic properties.

Experimental Section

Sample Preparation, STM/STS Measurement, and Raman Measurement: Experiments were carried out in an ultrahigh vacuum (base pressure of 1×10^{-10} mbar), low-temperature STM system (Unisoku), equipped with standard surface preparation facilities. The Ru(0001) (Mateck) surface was prepared by repeated cycles of Ar^+ sputtering and annealing at 950 °C. Large-area high-quality MLG was prepared via pyrolysis of ethylene on Ru(0001), as described elsewhere.[27,41] Hydrogenation of MLG/Ru(0001) was performed in a plasma chamber (background pressure of 5×10^{-9} mbar) using ultrahigh vacuum helical inductively coupled RF plasma[42] of 13.56 MHz at a power of 115 W. A gas mixture of H_2 (15%) and Ar (85%) at a pressure of 1×10^{-4} mbar was used. Although the presence of Ar gas in the mixture is not strictly necessary for the hydrogenation process, it was used due to safety considerations. An ion deflection voltage of 250 V was applied to get hydrogen atoms instead of H ions. STM images were acquired in constant-current mode, and all given voltages refer to the sample. Differential conductance (dI/dV) spectra were collected by using a lock-in technique with a 10 mV_{rms} sinusoidal modulation at a frequency of 973 Hz. All STM/STS experiments were performed with electrochemically etched tungsten tips at 4.2 K. Raman spectra were acquired by a Renishaw spectrometer at 532 nm with a lateral resolution of 1 µm.

First-Principles Calculations: The DFT calculations were performed with the Vienna Ab initio Simulation Package (VASP)[43] and the projector augmented wave (PAW)[44] method. Local density approximation (LDA)[45] in the form of Perdew–Zunger was adopted for the exchange-correlation functional for the structural optimization. The energy cutoff of the plane-wave basis set was 400 eV. The unit cell was chosen as a $\sqrt{3} \times \sqrt{3}$ superlattice of graphene, with two hydrogen atoms bonding to two neighboring C atoms at both sides. The thickness of the vacuum layer was 15 Å. Structural optimization was performed until the force on each atom was less than 0.01 eV $Å^{-1}$. The k-points sampling was $15 \times 15 \times 1$ and $45 \times 45 \times 1$ for structural relaxation and DOS calculations, respectively. The hybrid functional HSE06[46] was used to calculate the band structure and DOS of the OTHG. For ab initio

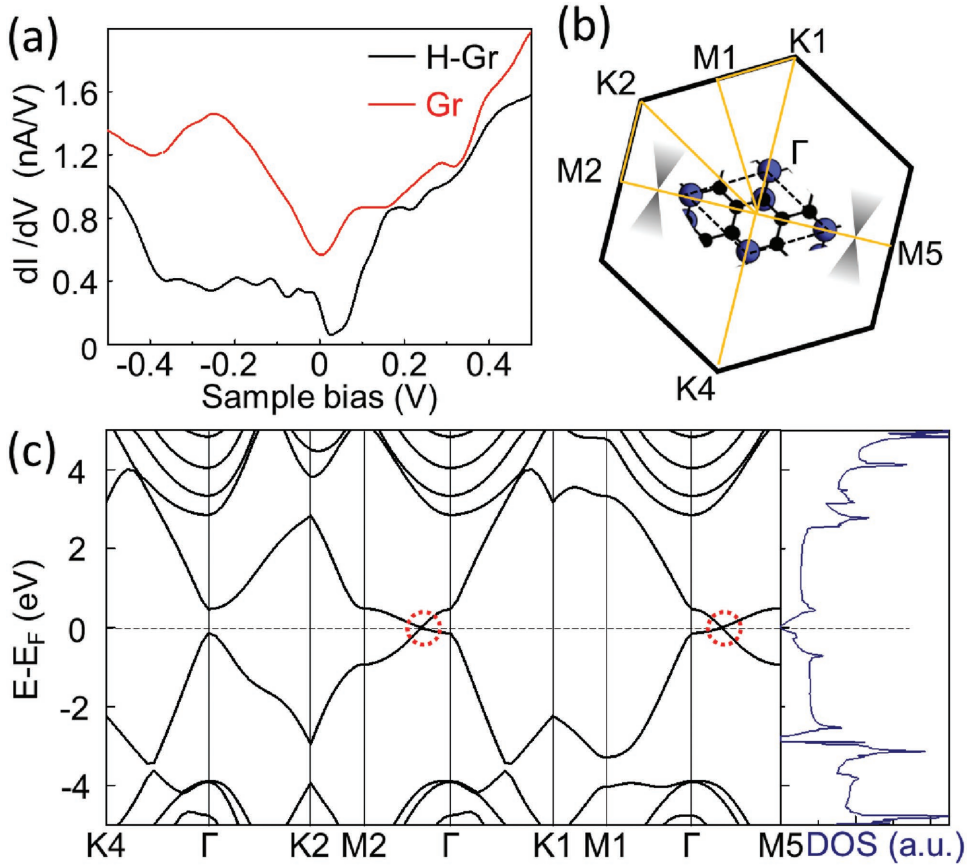

Figure 4. Electronic properties of the OTHG. a) A typical dI/dV spectrum of pristine graphene (red curve) and as-fabricated OTHG (black curve). The latter shows a decrease of the density of states in the range from –0.4 to 0.1 V and a sharp V-shaped dip around E_F. A dI/dV spectrum recorded on pristine graphene on Ru(0001) is also shown for comparison. ($U = -0.6$ V, $I = 0.1$ nA; lock-in modulation: $V_{rms} = 5$ mV). b) The first Brillouin zone and the high-symmetry directions of freestanding OTHG, corresponding to the configuration in Figure 2d. c) Calculated band structure (left panel) and total electronic density of states (right panel), using the HSE06 hybrid functional method, showing anisotropic electronic properties of the OTHG. The two Dirac cones at E_F along the high-symmetry Γ-M1 and Γ-M2 directions are indicated with red dashed rings.

molecular dynamics (AIMD) simulations, a canonical (*NVT*) ensemble was used at 1200 K. Time interval between each step is 0.5 fs.[47]

Supporting Information

Supporting Information is available from the Wiley Online Library or from the author.

Acknowledgements

H.C. and D.-L.B. contributed equally to this work. This work was financially supported by the National Natural Science Foundation of China (Nos. 61390501 and 51761135130), National "973" projects of China (2013CBA01600), National Key Research and Development Projects of China (2016YFA0202300 and 2016YFA0300904), Strategic Priority Research Program of the Chinese Academy of Sciences (CAS) (Nos. XDPB0601, XDB07030100, and XDPB08-1), the CAS Pioneer Hundred Talents Program, and Beijing Nova Program (No. Z181100006218023). Work at Vanderbilt (S.T.P., Y.-Y.Z., and D.-L.B.) was supported by the U.S. Department of Energy under Grant No. DE-FG02-09ER46554 and by the McMinn Endowment. Computations by Y.-Y.Z. and S.T.P. were carried out at the National Energy Research Scientific Computing Center, a DOE Office of Science User Facility supported by the Office of Science of the U.S. Department of Energy under Contract No. DE-AC02-05CH11231. Computations by D.-L.B. were carried out at the National Supercomputing Center of Tianjin.

Conflict of Interest

The authors declare no conflict of interest.

Keywords

anisotropy, hydrogenated graphene, millimeter-scale, single crystals

Received: March 22, 2018
Revised: May 2, 2018
Published online: June 25, 2018

[1] H. Bai, C. Li, G. Q. Shi, *Adv. Mater.* **2011**, *23*, 1089.
[2] L. Liao, Q. Xie, X. F. Guo, Z. F. Liu, *Adv. Mater.* **2015**, *27*, 4093.
[3] L. Zhou, L. Liao, J. Y. Wang, J. W. Yu, D. H. Li, Q. Xie, Z. R. Liu, Y. L. Yang, X. F. Guo, Z. F. Liu, *Adv. Mater.* **2016**, *28*, 2148.

[4] M. Zeng, Y. Xiao, J. Liu, W. Lu, L. Fu, *Adv. Electron. Mater.* **2016**, *2*, 1500456.
[5] G. D. Nguyen, H.-Z. Tsai, A. A. Omrani, T. Marangoni, M. Wu, D. J. Rizzo, G. F. Rodgers, R. R. Cloke, R. A. Durr, Y. Sakai, *Nat. Nanotechnol.* **2017**, *12*, 1077.
[6] M. Zeng, Y. Xiao, J. Liu, K. Yang, L. Fu, *Chem. Rev.* **2018**, https://doi.org/10.1021/acs.chemrev.7b00633.
[7] M. Lozada-Hidalgo, S. Zhang, S. Hu, V. G. Kravets, F. J. Rodriguez, A. Berdyugin, A. Grigorenko, A. K. Geim, *Nat. Nanotechnol.* **2018**, *13*, 300.
[8] L. L. Patera, F. Bianchini, C. Africh, C. Dri, G. Soldano, M. M. Mariscal, M. Peressi, G. Comelli, *Science* **2018**, *359*, 1243.
[9] D. C. Elias, R. R. Nair, T. M. G. Mohiuddin, S. V. Morozov, P. Blake, M. P. Halsall, A. C. Ferrari, D. W. Boukhvalov, M. I. Katsnelson, A. K. Geim, K. S. Novoselov, *Science* **2009**, *323*, 610.
[10] J. Balakrishnan, G. K. W. Koon, M. Jaiswal, A. H. C. Neto, B. Ozyilmaz, *Nat. Phys.* **2013**, *9*, 284.
[11] R. Balog, B. Jørgensen, L. Nilsson, M. Andersen, E. Rienks, M. Bianchi, M. Fanetti, E. Laegsgaard, A. Baraldi, S. Lizzit, Z. Sljivancanin, F. Besenbacher, B. Hammer, T. G. Pedersen, P. Hofmann, L. Hornekaer, *Nat. Mater.* **2010**, *9*, 315.
[12] H. González-Herrero, J. M. Gómez-Rodríguez, P. Mallet, M. Moaied, J. J. Palacios, C. Salgado, M. M. Ugeda, J.-Y. Veuillen, F. Yndurain, I. Brihuega, *Science* **2016**, *352*, 437.
[13] H. L. Gao, L. Wang, J. J. Zhao, F. Ding, J. P. Lu, *J. Phys. Chem. C* **2011**, *115*, 3236.
[14] M. Yang, A. Nurbawono, C. Zhang, Y. P. Feng, Ariando, *Appl. Phys. Lett.* **2010**, *96*, 193115.
[15] J. O. Sofo, A. S. Chaudhari, G. D. Barber, *Phys. Rev. B* **2007**, *75*, 153401.
[16] J. Zhou, Q. Wang, Q. Sun, X. S. Chen, Y. Kawazoe, P. Jena, *Nano Lett.* **2009**, *9*, 3867.
[17] H. Y. Lu, A. S. Cuamba, L. Geng, L. Hao, Y. M. Qi, C. S. Ting, *Phys. Rev. B* **2017**, *96*, 165420.
[18] H. Y. Lu, A. S. Cuamba, S. Y. Lin, L. Hao, R. Wang, H. Li, Y. Y. Zhao, C. S. Ting, *Phys. Rev. B* **2016**, *94*.195423.
[19] Y. F. Li, Z. F. Chen, *J. Phys. Chem. C* **2012**, *116*, 4526.
[20] W. K. Lee, K. E. Whitener, J. T. Robinson, P. E. Sheehan, *Adv. Mater.* **2015**, *27*, 1774.
[21] W. Zhao, J. Gebhardt, F. Spath, K. Gotterbarm, C. Gleichweit, H. P. Steinruck, A. Gorling, C. Papp, *Chem. - Eur. J.* **2015**, *21*, 3347.
[22] S. J. Tjung, S. M. Hollen, G. A. Gambrel, N. M. Santagata, E. Johnston-Halperin, J. A. Gupta, *Carbon* **2017**, *124*, 97.
[23] D. Haberer, C. E. Giusca, Y. Wang, H. Sachdev, A. V. Fedorov, M. Farjam, S. A. Jafari, D. V. Vyalikh, D. Usachov, X. J. Liu, U. Treske, M. Grobosch, O. Vilkov, V. K. Adamchuk, S. Irle, S. R. P. Silva, M. Knupfer, B. Buchner, A. Gruneis, *Adv. Mater.* **2011**, *23*, 4497.
[24] J. H. Jorgensen, A. G. Cabo, R. Balog, L. Kyhl, M. N. Groves, A. M. Cassidy, A. Bruix, M. Bianchi, M. Dendzik, M. A. Arman, L. Lammich, J. I. Pascual, J. Knudsen, B. Hammer, P. Hofmann, L. Hornekaer, *ACS Nano* **2016**, *10*, 10798.
[25] C. Lin, Y. Feng, Y. Xiao, M. Durr, X. Huang, X. Xu, R. Zhao, E. Wang, X. Z. Li, Z. Hu, *Nano Lett.* **2015**, *15*, 903.
[26] Y. Wang, X. F. Xu, J. Lu, M. Lin, Q. L. Bao, B. Ozyilmaz, K. P. Loh, *ACS Nano* **2010**, *4*, 6146.
[27] Y. Pan, H. Zhang, D. Shi, J. Sun, S. Du, F. Liu, H.-J. Gao, *Adv. Mater.* **2009**, *21*, 2777.
[28] Y. Pan, L. Z. Zhang, L. Huang, L. F. Li, L. Meng, M. Gao, Q. Huan, X. Lin, Y. L. Wang, S. X. Du, H. J. Freund, H.-J. Gao, *Small* **2014**, *10*, 2215.
[29] J. D. Ren, H. M. Guo, J. B. Pan, Y. Y. Zhang, X. Wu, H. G. Luo, S. X. Du, S. T. Pantelides, H.-J. Gao, *Nano Lett.* **2014**, *14*, 4011.
[30] J. Ren, H. Guo, J. Pan, Y.-F. Zhang, Y. Yang, X. Wu, S. Du, M. Ouyang, H.-J. Gao, *Phys. Rev. Lett.* **2017**, *119*, 176806.
[31] J. Mao, H. Zhang, Y. Jiang, Y. Pan, M. Gao, W. Xiao, H.-J. Gao, *J. Am. Chem. Soc.* **2009**, *131*, 14136.
[32] P. W. Sutter, J. I. Flege, E. A. Sutter, *Nat. Mater.* **2008**, *7*, 406.
[33] M. Hupalo, X. J. Liu, C. Z. Wang, W. C. Lu, Y. X. Yao, K. M. Ho, M. C. Tringides, *Adv. Mater.* **2011**, *23*, 2082.
[34] L. Meng, R. Wu, H. Zhou, G. Li, Y. Zhang, L. Li, Y. Wang, H.-J. Gao, *Appl. Phys. Lett.* **2012**, *100*, 083101.
[35] X. Fei, L. Zhang, W. Xiao, H. Chen, Y. Que, L. Liu, K. Yang, S. Du, H.-J. Gao, *J. Phys. Chem. C* **2015**, *119*, 9839.
[36] D. Yi, L. Yang, S. J. Xie, A. Saxena, *RSC Adv.* **2015**, *5*, 20617.
[37] D. W. Boukhvalov, M. I. Katsnelson, A. I. Lichtenstein, *Phys. Rev. B* **2008**, *77*, 035427.
[38] P. Sutter, J. T. Sadowski, E. A. Sutter, *J. Am. Chem. Soc.* **2010**, *132*, 8175.
[39] C. Riedl, C. Coletti, T. Iwasaki, A. A. Zakharov, U. Starke, *Phys. Rev. Lett.* **2009**, *103*, 246804.
[40] C.-H. Park, L. Yang, Y.-W. Son, M. L. Cohen, S. G. Louie, *Nat. Phys.* **2008**, *4*, 213.
[41] Y. Pan, D. Shi, H.-J. Gao, *Chin. Phys.* **2007**, *16*, 3151.
[42] R. Yang, L. Zhang, Y. Wang, Z. Shi, D. Shi, H. Gao, E. Wang, G. Zhang, *Adv. Mater.* **2010**, *22*, 4014.
[43] D. Vanderbilt, *Phys. Rev. B* **1990**, *41*, 7892.
[44] G. Kresse, D. Joubert, *Phys. Rev. B* **1999**, *59*, 1758.
[45] J. P. Perdew, A. Zunger, *Phys. Rev. B* **1981**, *23*, 5048.
[46] A. V. Krukau, O. A. Vydrov, A. F. Izmaylov, G. E. Scuseria, *J. Chem. Phys.* **2006**, *125*, 224106.
[47] G. Kresse, J. Hafner, *Phys. Rev. B* **1993**, *47*, 558.